

Ca²⁺/CaM dependent protein kinase II (CaMKII) α and CaMKII β hub domains adopt distinct oligomeric states and stabilities

Can Özden^{1,2}  | Sara MacManus¹ | Ruth Adafia^{1,2} | Alfred Samkutty¹ | Ana P. Torres-Ocampo^{1,2} | Scott C. Garman¹ | Margaret M. Stratton¹ 

¹Department of Biochemistry and Molecular Biology, University of Massachusetts, Amherst, Massachusetts, USA

²Molecular and Cellular Biology Graduate Program, University of Massachusetts, Amherst, Massachusetts, USA

Correspondence

Margaret M. Stratton, Department of Biochemistry and Molecular Biology, University of Massachusetts, Amherst, MA, USA.

Email: mstratton@umass.edu

Funding information

National Institute of General Medical Sciences; R35GM145376

Review Editor: Aitziber L. Cortajarena

Abstract

Ca²⁺/calmodulin-dependent protein kinase II (CaMKII) is a multidomain serine/threonine kinase that plays important roles in the brain, heart, muscle tissue, and eggs/sperm. The N-terminal kinase and regulatory domain is connected by a flexible linker to the C-terminal hub domain. The hub domain drives the oligomeric organization of CaMKII, assembling the kinase domains into high local concentration. Previous structural studies have shown multiple stoichiometries of the holoenzyme as well as the hub domain alone. Here, we report a comprehensive study of the hub domain stoichiometry and stability in solution. We solved two crystal structures of the CaMKII β hub domain that show 14-mer (3.1 Å) and 16-mer (3.4 Å) assemblies. Both crystal structures were determined from crystals grown in the same drop, which suggests that CaMKII oligomers with different stoichiometries likely coexist. To further interrogate hub stability, we employed mass photometry and temperature denaturation studies of CaMKII β and CaMKII α hubs, which highlight major differences between these highly similar domains. We created a dimeric CaMKII β hub unit using rational mutagenesis, which is significantly less stable than the oligomer. Both hub domains populate an intermediate during unfolding. We found that multiple CaMKII β hub stoichiometries are present in solution and that larger oligomers are more stable. CaMKII α had a narrower distribution of molecular weight and was distinctly more stable than CaMKII β .

KEYWORDS

CaMKII, oligomerization domain, protein folding, stoichiometry

1 | INTRODUCTION

Ca²⁺/calmodulin-dependent protein kinase II (CaMKII) is a serine/threonine kinase that is crucial to memory formation, cardiac pacemaking, and fertilization. The

unique multimeric structure of CaMKII is driven by the C-terminal hub domain. The N-terminal kinase domain is tethered to the hub domain through a regulatory segment and flexible linker. The hub domains assemble as two stacked rings, which form the core of the CaMKII holoenzyme (Bhattacharyya et al., 2019; Chao et al., 2011). CaMKII is highly conserved across species,

Can Özden and Sara MacManus contributed equally.

with the exception of the linker region, and is expressed by four paralogous genes in humans (α , β , δ , and γ) (Sloutsky & Stratton, 2020; Tombes et al., 2003). CaMKII is a metazoan protein, and homologs of full-length CaMKII have been found in choanoflagellates (Bhattacharyya et al., 2016). Homologs of the CaMKII hub domain have also been found in bacteria and plants (McSpadden et al., 2019).

Structural studies have shown that each ring of the hub domain has 6 to 8 subunits, forming oligomers with 12 to 16 total subunits (Bhattacharyya et al., 2016; Hoelz et al., 2003; Kolodziej et al., 2000; McSpadden et al., 2019; Morris & Torok, 2001; Rellos et al., 2010; Rosenberg et al., 2006). To date, the human and mouse CaMKII hub domains of α , δ , and γ have been crystallized as either 12- or 14-mer complexes (Bhattacharyya et al., 2016; Hoelz et al., 2003; Rellos et al., 2010). A CaMKII hub-like protein from *Chlamydomonas reinhardtii* has been crystallized as an 18-mer complex, which indicates the possibility of higher stoichiometries (McSpadden et al., 2019). Upon comparative analysis, it has been proposed that different stoichiometries are facilitated by the changes in beta sheet curvature and/or additional intrachain hydrogen bonds (McSpadden et al., 2019). A recent study revealed a putative model of the first 16-mer complex of a CaMKII β holoenzyme using negative stain electron microscopy (EM) (Buonarati et al., 2021). The same study showed that both CaMKII α and CaMKII β holoenzymes form mostly 12-mers along with a lower population of 14-mers.

Mass photometry (MP) measures the molecular weight of single particles in solution (Sonn-Segev et al., 2020; Young et al., 2018). This technique has been used to show that CaMKII α holoenzymes in solution cluster around a molecular weight of a 10 to 12-mer (Lucic et al., 2023; Torres-Ocampo et al., 2020), whereas the CaMKII α hub domains form larger species, around 16-mers (Torres-Ocampo et al., 2020). The CaMKII α hub domain is significantly more stable than the CaMKII α holoenzyme in terms of temperature stability and oligomerization (Leurs et al., 2021; Torres-Ocampo et al., 2020). Another study measured the melting temperature of the monomeric *Caenorhabditis elegans* CaMKII variant to be roughly 63°C (Hoffman et al., 2011). Overall, the stability of CaMKII variants has been largely understudied.

Here, we report two human CaMKII β hub domain crystal structures at <3.5 Å with 14- and 16-mer stoichiometries. We use MP and circular dichroism (CD) to interrogate the stoichiometry and stability in solution of the CaMKII β hub domain, and we compared this to the CaMKII α hub. It has been previously shown that the hub domain impacts CaMKII activity (Roman Sloutsky et al., 2020), so it is important to consider distinctions

between variants in understanding how stoichiometry and hub dynamics impact CaMKII regulation.

2 | RESULTS

2.1 | Two CaMKII β hub stoichiometries from a single crystallization drop

Initial CaMKII β hub crystals were canoe shaped (Figure 1a). A 14-mer hub structure was determined at 3.1 Å resolution using a data set collected from a crystal on the right side of the drop (Figure 1a,b, PDB: 7URW). The space group (C222₁) and unit cell dimensions (104.24, 183.19, 108.37) of this structure are comparable to a recently published CaMKII α hub 14-mer (PDB: 7REC) (Buonarati et al., 2021). Crystal packing and oligomer dimensions (112 Å × 112 Å × 60 Å, Figure 1b,c; Table 1) of both structures are nearly identical.

Two days later, crystals with a different morphology (tetragonal bipyramid with 4-fold symmetry), as well as many microcrystals, appeared in the same drop (Figure 1d). From these crystals, we determined a 16-mer structure at 3.4 Å resolution (PDB: 7URZ). There are four hub domains in the asymmetric unit cell with a P4 symmetry. The space group (P4₂2₁2) and unit cell dimensions (81.34, 81.34, 180.04) are distinct from the tetradecameric structure. Comparing this 16-mer hub structure to the hub of the 16-mer holoenzyme EM structure (Rosenberg et al., 2006), the outer diameter measurements are comparable (128 Å × 125 Å × 62 Å, Figure 1e,f; Table 1).

In the structures presented here, the curvature of the central β -sheets changes with stoichiometry, as described previously (Figure 1g) (McSpadden et al., 2019). The difference in angle between β -sheets in CaMKII α 12-mer compared with a 14-mer is $\sim 8.6^\circ$ (Bhattacharyya et al., 2016). The difference in angle is closer to 3° when we compared the 14- and 16-mer CaMKII β hubs. We would expect that as ring size increases, the angle between subunits will not change as drastically. The 16-mer is subtly larger in all dimensions compared to 14-mer (Figure 1c,f). Comparison of the inside cavities shows that the 16-mer structure has an elliptical cavity (36 Å × 40 Å), whereas the 14-mer structure cavity is circular (25 Å × 25 Å, Figure 1b,e).

The C terminus of each hub domain extends from the final β -sheet (β_6), which faces the central pore of the donut (Figure S1a). The construct used for the CaMKII β hub structures presented here includes all C-terminal residues, but the last 3 to 5 residues are only well resolved in 1 out of 11 unique chains between the two structures. We compared an additional 14-mer

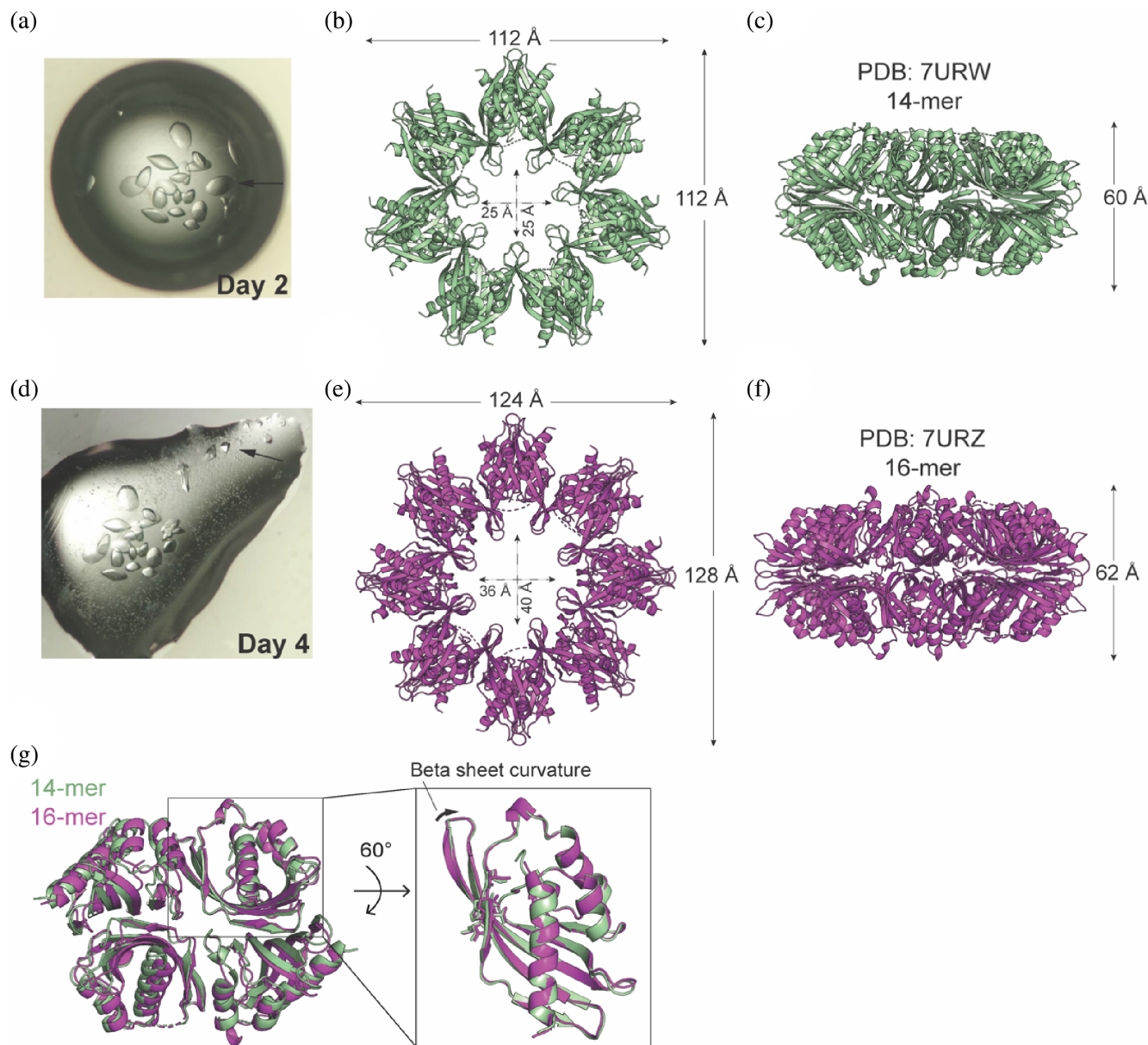


FIGURE 1 Two CaMKII β hub domain stoichiometries from one crystallization drop. (a) Protein crystals shown at the two-day timepoint. The arrow indicates the crystal used for data collection of crystal structure presented in (b). A 14-mer hub domain crystal structure (PDB code: [7URW](#)) shown (b) top-view and (c) side-view. (d) Protein crystals with different morphology appeared in the same drop at the four-day timepoint. The arrow indicates the crystal used for data collection of crystal structure presented in (e). A 16-mer CaMKII β hub domain crystal structure (PDB code: [7URZ](#)) shown (e) top-view, (f) side-view. (g) Overlay of tetramers from 14-mer (green, PDB: [7URW](#)) and 16-mer (magenta, PDB: [7URZ](#)) structures. On the left, a tetramer of the hub domains is shown. Structures are aligned along the core α -helix and the first β -sheet of the domain in the box. The inset shows an orientation of the subunit where the curvature is highlighted, as evidenced by the offset of residues highlighted as sticks for clarity. Increased beta sheet curvature facilitates larger ring formation. CaMKII, Ca²⁺/calmodulin-dependent protein kinase II.

CaMKII β hub structure deposited at higher resolution (2.6 Å, PDB code: [7URY](#)) (Saha et al., 2023), where the last three to five residues are resolved in five out of seven unique chains. We observe that these terminal residues fold back toward the central pocket of their own hub domain (Figure S1a). Two proline residues facilitate turns at the C terminus (Figure S1b,c).

2.2 | CaMKII β hub stability

Since multiple stoichiometries can be formed in crystals, we sought to interrogate stoichiometry and its effects on stability in solution. We performed differential scanning calorimetry on the CaMKII β hub, which showed an apparent melting temperature (T_m) of 102.2°C

TABLE 1 The 14- and 16-mer CaMKII β hub domain crystal structures.

| | 14-mer CaMKII β hub domain (PDB:7URW) | 16-mer CaMKII β hub domain (PDB:7URZ) |
|---------------------------------------|---|---|
| Data collection | | |
| Space group | $C222_1$ | $P4_22_12$ |
| Cell dimensions | | |
| a, b, c (Å) | 104.24, 183.19, 108.37 | 81.34, 81.34, 180.04 |
| α, β, γ (°) | 90, 90, 90 | 90, 90, 90 |
| Resolution (Å) | 50–3.1 (3.15–3.1) | 60–3.45 (3.53–3.47) |
| R_{merge} | 0.291 (1.454) | 0.368 (1.361) |
| Mean $I/\sigma I$ | 6.2 (1.67) | 4.5 (2.02) |
| Completeness (%) | 98.5 (95.4) | 99.2 (99.0) |
| Redundancy | 6.2 (5.5) | 7.3 (7.5) |
| $CC_{1/2}$ | 0.962 (0.567) | 0.992 (0.650) |
| CC^* | 0.990 (0.851) | 0.998 (0.888) |
| Refinement | | |
| Resolution (Å) | 37.8–3.11 (3.186–3.11) | 37.09–3.45 (3.537–3.45) |
| Unique reflections | 17,703 (1200) | 7921 (578) |
| $R_{\text{work}}/R_{\text{free}}$ (%) | 25.7/30.02 | 35.44/40.74 |
| No. of atoms | | |
| Protein | 6789 | 3910 |
| Water | - | - |
| Ligand | - | - |
| Ramachadran plot | | |
| In preferred regions (%) | 97.54 | 95.16 |
| In allowed regions (%) | 1.75 | 4.44 |
| Outliers (%) | 0.70 | 0.40 |
| B factors | | |
| Protein | 74.74 | 108.92 |
| Water | - | - |
| Ligand | - | - |
| R.M.S. deviations | | |
| Bond lengths (Å) | 0.0046 | 0.0022 |
| Bond angles (°) | 1.3269 | 1.1924 |

Abbreviation: CaMKII, Ca²⁺/calmodulin-dependent protein kinase II. R.M.S., root mean squared, CC., Pearson correlation coefficient

(Figure S2a). We then used CD to measure protein unfolding, and, as expected from the DSC data, a standard temperature melt to 100°C did not completely unfold the protein (Figure S2b). We performed the temperature melt in the presence of 2 M guanidine hydrochloride (GdnHCl) and observed two distinct, cooperative unfolding transitions (Figure 2a). This process was irreversible, so all values reported here are phenomenological (Figure S3a,b). The first transition ($N \rightleftharpoons I$) had a T_m of 56.5°C and a slope of $0.18 \pm 0.04 \text{ cal mol}^{-1} \text{ °C}^{-1}$. The second transition ($I \rightleftharpoons U$) had a T_m of 81.8°C and a slope of $0.35 \pm 0.06 \text{ cal mol}^{-1} \text{ °C}^{-1}$ (Table 2). We also performed guanidine melts on the CaMKII β hub (Figure 2b). The oligomer is fully unfolded at 4.5 M GdnHCl and evidently transitions through an intermediate, but these data were not easily fitted to a 2- or 3-state equation.

2.3 | Defining the unfolding mechanism

We utilized mass photometry (MP) to determine the oligomeric state of the CaMKII β hub during the unfolding process. We performed MP measurements of samples collected along the unfolding trajectory as shown in Figure 2a, sampling temperatures representing each state along the unfolding pathway in the presence of 2 M GdnHCl (25°C, 40°C, 70°C, and 97°C) (Figure 2c; Figure S4a–c). Since MP is performed at significantly lower concentrations, we verified that a dilution series maintains the same populations with and without GdnHCl (Figure S5a,b). At all temperatures, there is a small population around 75 kDa. Control measurements indicated that this is partially contributed by guanidine and likely partially contributed by lower-order species or unfolded monomers (Figure S4d). Before the first transition (25°C and 40°C), there are two distinct CaMKII β hub populations that represent ~ 12 - and ~ 14 -mers. The lower mass peaks are centered around $191 \pm 16.5 \text{ kDa}$ (25°C) and $193 \pm 15.6 \text{ kDa}$ (40°C), which correspond to 12-mers (180 kDa) along with a small population of 14-mers (210 kDa). The higher mass peaks are centered around $218 \pm 19.2 \text{ kDa}$ (25°C) and $230 \pm 17.7 \text{ kDa}$ (40°C), which correspond to a mixture of 14-mers (210 kDa) and 16-mers (240 kDa). Notably, there is a population shift from 218 kDa to 230 kDa between 25°C and 40°C, indicating that the larger species are selected for at higher temperatures. After the first unfolding transition (70°C), the lower mass oligomeric peak disappears and a single peak with a mass of $226 \pm 16.0 \text{ kDa}$ is observed, representing a mixture of 14- and 16-mers.

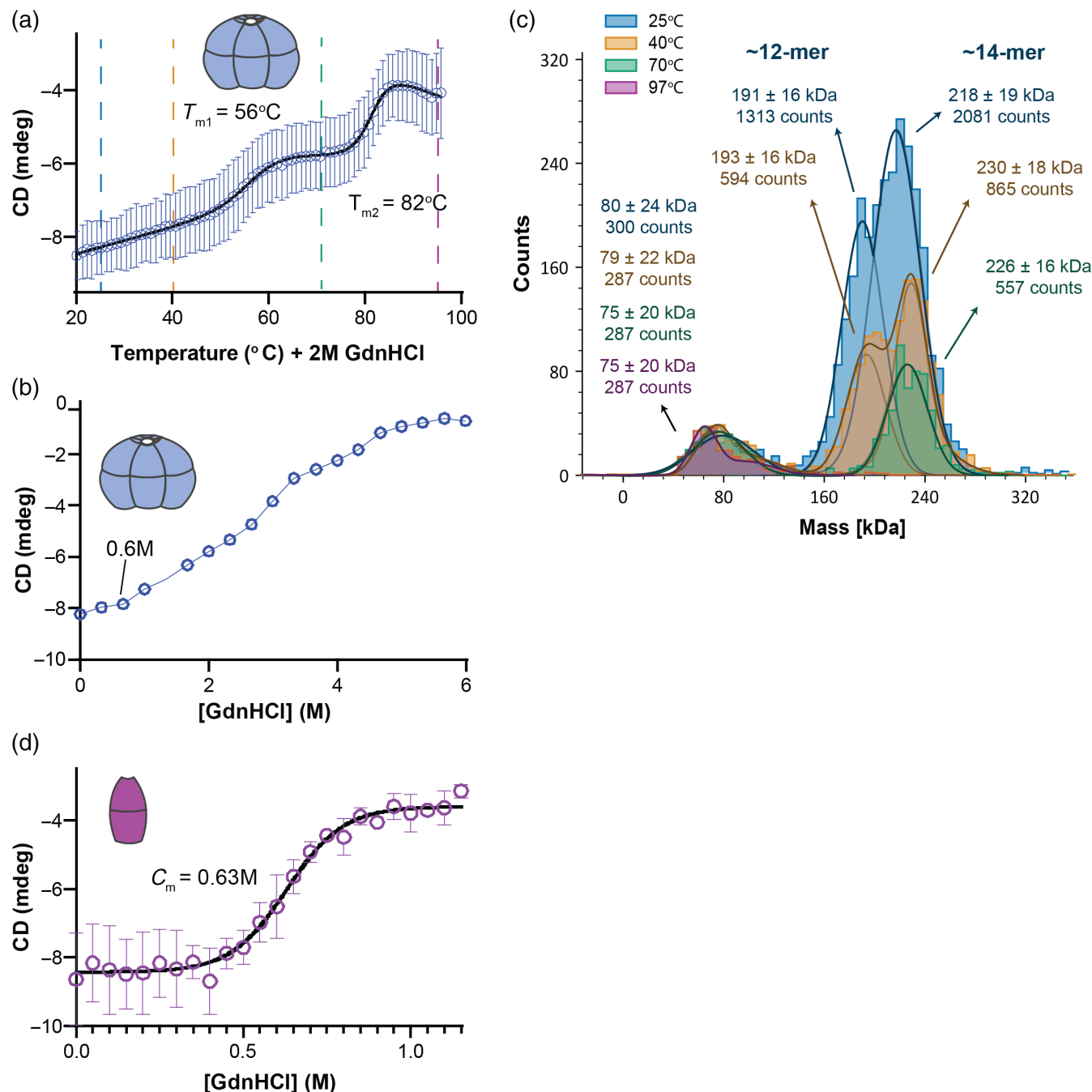


FIGURE 2 CaMKII β hub unfolding. (a) Temperature melt of CaMKII β hub oligomer in the presence of 2 M guanidine hydrochloride (GdnHCl). Data points represent average circular dichroism (CD) signal at 218 nm ($n = 9$). Data are fit to a 3-state non-linear regression. Vertical dashed lines indicate temperatures at which mass photometry (MP) measurements were performed (c). (b) Guanidine melt of CaMKII β hub oligomer. Blue data points represent average CD signal at 218 nm ($n = 9$). (c) Representative MP histogram for CaMKII β hub samples ($n = 8$) that have been incubated in 2 M GdnHCl and heated to the indicated temperature. Each count indicates a single molecule. (d) Guanidine melt of CaMKII β hub dimer mutant (F585A + L622M). Data points represent average CD signal at 218 nm ($n = 9$). Data are fit to a 2-state non-linear regression. CaMKII, Ca²⁺/calmodulin-dependent protein kinase II.

After the second unfolding transition (97°C), no oligomeric peaks remain. We cannot measure whether the proteins are all monomeric at 97°C (the resolution of the Refeyn One MP cannot detect individual hub monomers of 15 kDa), but it is likely that all hub domains have

fully unfolded because the CD shows all secondary structure was melted at this temperature (Figure 2a; Figure S3b).

Since MP can distinguish larger species but not smaller ones, we wanted to use a different technique to assess

| | Slope (kcal mol ⁻¹ K ⁻¹) | ΔG_{app} (kcal mol ⁻¹) | T_m (°C) |
|--------------------------|---|---|----------------|
| N \rightleftharpoons I | 0.18 \pm 0.04 | 10 \pm 2 | 56.5 \pm 1.9 |
| I \rightleftharpoons U | 0.35 \pm 0.06 | 28 \pm 5 | 81.8 \pm 1.4 |

TABLE 2 Thermodynamic parameters for N \rightleftharpoons I and I \rightleftharpoons U transitions.

Note: Mean and standard deviation for the calculated slope, ΔG_{app} , and T_m for the two transitions observed in the temperature melt; $n = 9$.

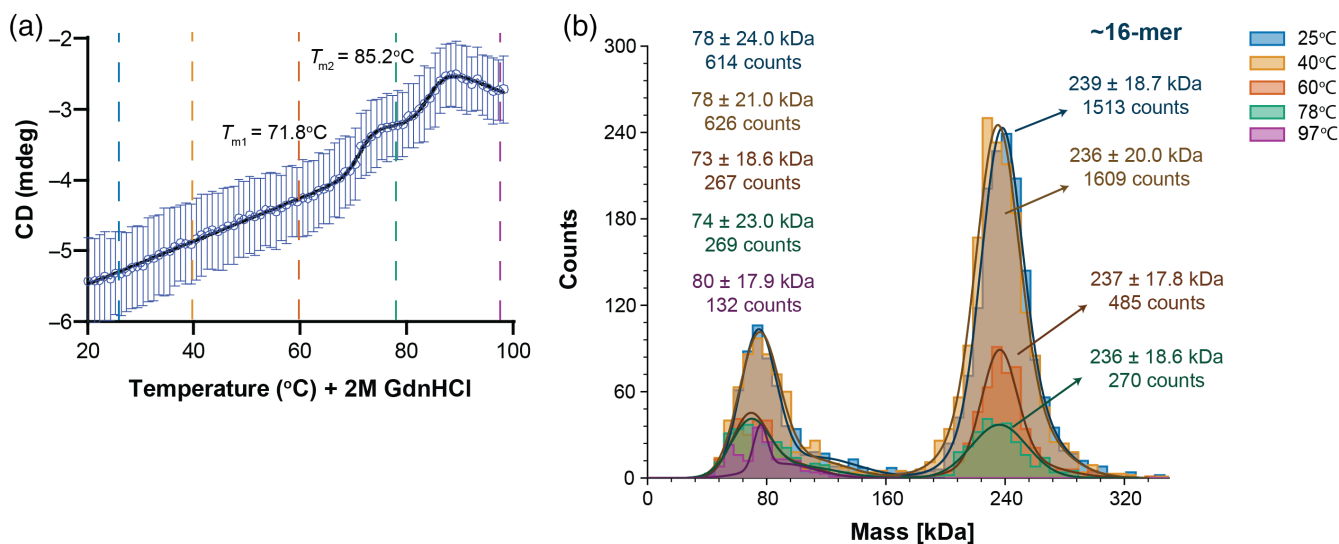


FIGURE 3 CaMKII α hub unfolding. (a) Temperature melt of CaMKII α hub oligomer with 2 M guanidine hydrochloride (GdnHCl). Blue data points represent average circular dichroism (CD) signal at 218 nm ($n = 6$). Data are fit to a 3-state non-linear regression. Vertical dashed lines indicate temperatures at which mass photometry (MP) measurements were performed (b). (b) Representative MP histogram for CaMKII α hub samples ($n = 6$) that have been incubated in 2 M GdnHCl and heated to the indicated temperature. Each count indicates a single molecule. Note that the 25°C population (blue) is overlapping with the 40°C population (yellow). CaMKII, Ca²⁺/calmodulin-dependent protein kinase II.

the stability of a smaller hub unit. There is mounting evidence that upon dissociation, CaMKII releases vertical dimer units (Sarkar et al., 2017; Stratton et al., 2014). We designed a double mutant (F585A + L622M) that disrupts the lateral interfaces in the CaMKII β hub domain to form predominantly vertical dimers. A single mutation has not sufficed to eliminate all oligomerization in solution (Bhattacharyya et al., 2016; Sarkar et al., 2017). Size-exclusion chromatography paired with multiangle light scattering confirmed that the double-mutant we created (herein referred to as dimer) migrated as a single peak and had a calculated mass of around 36 kDa, whereas the wild-type (WT) hub domain had two mass peaks: 207 and 176 kDa (Figure S6a). This confirmed our double-mutant forms only dimers in solution. Additionally, the CD signatures of the dimer and the WT hub overlap well, indicating that these mutations do not affect monomer folding (Figure S6b). We performed a guanidine melt on the dimer, which gave a C_m of 0.63 M GdnHCl (Figure 2d). We directly compared the unfolding of the CaMKII β hub oligomer to that of the hub dimer and observed that the oligomer starts to unfold around

90°C, whereas the dimer is completely unfolded by 60°C ($T_m = 51.7$) (Figure S2b,c).

2.4 | CaMKII α hub displays differences in stability compared with CaMKII β hub

CaMKII α and CaMKII β hub domains share 77% sequence identity—but do they act similarly in solution? In MP measurements, the CaMKII α hub formed a single population centered at a 16-mer size (240 kDa), as opposed to the two populations observed for the CaMKII β hub (Figures S7 and S8). We performed temperature denaturation melts on the CaMKII α hub in the presence of 2 M GdnHCl. This showed two unfolding transitions, with T_m values of 71.8°C and 85.2°C (Figure 3a), both higher than those of the CaMKII β hub unfolding (see Figure 2a). We performed MP on the CaMKII α hub samples at temperatures before and after each transition (Figure 3b). The single population of the CaMKII α hub decreased in number across each transition (from 60°C to 90°C), indicating oligomer dissociation

and unfolding. However, there is no clear change in stoichiometry of the oligomer population across transitions nor an emergence of new populations that would directly account for the two separate transitions.

3 | DISCUSSION

The CaMKII holoenzyme is assembled by the hub domain, which oligomerizes to form a donut-like structure. The N-terminus of the hub domain forms a helix which connects to the catalytic domain in the full-length holoenzyme on the outside of the donut (Figure S1a). If the C-terminus was extended, it is unclear where these residues would travel to—this is an important factor to consider with fusion proteins and tags added at the C-terminal end of CaMKII. Of note, CaMKII δ has an extended C-terminus, which will likely have distinct effects on hub dynamics and stability. Each hub domain harbors a central pocket, which is lined with arginine residues. A previous study determined a structure of the CaMKII α hub domain bound to an analog of γ -hydroxybutyrate (5-HDC) in this arginine pocket and showed that this compound bound specifically to CaMKII α (Leurs et al., 2021). Other hub structures also trap molecules in this pocket, for example the other 14-mer CaMKII β hub structure (PDB code: 7URY) shows malic acid bound in the pocket (Saha et al., 2023). The specificity for 5-HDC is striking, and rather remarkable, given the high sequence conservation between CaMKII variants. A major difference between the hub domains is that in CaMKII α , there are three arginines in the pocket, whereas in CaMKII β , there are only two, and the third is substituted with cysteine (Figure S1b,c). Another difference is the sequence of the five C-terminal residues (Figure S1c), where both segments would be flexible but the sequences are different. As noted, our constructs have full-length C-termini compared with other CaMKII α structures which are terminated early; this may also affect stoichiometry and it will be important to interrogate this further.

We were intrigued to capture two distinct oligomeric states grown within the same crystallization drop, suggesting that these species coexist and/or interconvert. Although the biological implications of stoichiometry are not clear, it is possible that these allowable conformations lend CaMKII its unique properties such as subunit exchange (Bhattacharyya et al., 2016; Stratton et al., 2014). A recent study has shown that CaMKII β has different activation properties compared with CaMKII α (Roman Sloutsky et al., 2020). CaMKII α requires higher concentrations of Ca²⁺/calmodulin for activation, whereas CaMKII β was active at much lower

concentrations. This difference may be attributed to different stoichiometric states.

Both CaMKII α and β hub domains are extremely stable, requiring temperatures of over 90°C for unfolding (Torres-Ocampo et al., 2020). In fact, in order to observe unfolding in an achievable temperature range, we needed to add denaturant (2 M GdnHCl). Surprisingly, both hub domains unfolded in a 3-state reaction, but these reactions are distinct from one another despite the high sequence similarity between these domains (Figure S8a). CaMKII β hub undergoes its first unfolding transition at a lower temperature compared with CaMKII α . From MP measurements, we interpret this first transition as the 12-mer oligomers unfolding, while the 14/16-mer oligomers remain (Figure S8a–e). The second transition is the remaining 14/16-mer oligomers dissociating and unfolding. We interpret this to mean that the 14/16-mer population is more stable; the 14/16-mer has more buried interfaces, suggesting that this stability can be attributed to favorable enthalpic contributions provided by the higher oligomeric state. The CaMKII α unfolding mechanism appears to be more nuanced, as the oligomeric state (16-mer) does not obviously change during unfolding. A possible explanation for the first unfolding transition (71°C) is that the oligomeric ring cracks at one vertical interface, creating a spiraled ring which has been previously reported (Bhattacharyya et al., 2016). The second transition would then be all spiraled oligomers dissociating and unfolding. It is also notable that the CaMKII α transitions (closed to open ring/dissociation and unfolding) are closer energetically ($\Delta 13^\circ\text{C}$) compared with the transitions for CaMKII β ($\Delta 26^\circ\text{C}$). The second transition for CaMKII α and CaMKII β hubs is overlapping (Figure S8a), it is possible that full dissociation and unfolding are the same energetically for both variants.

The molar ellipticity of the hub dimer we created is the same as that of the oligomer, so any change in CD signal observed during the denaturation is likely attributed to monomer unfolding rather than disassembly into dimers. Both hub domains displayed a large native baseline slope over the first 40–60 degrees of the experiment. We interpret this slope as oligomers (regardless of stoichiometry) disassembling into dimers and unfolding immediately (Figure 4a), which is reflected in the MP measurements where the oligomeric peak(s) counts decrease steadily over this temperature range (Figures 2c and 3b). We cannot rule out precipitation occurring during the measurement; however, we do not observe any large species in MP. We were unable to fit the GdnHCl melt of the CaMKII β hub domain to a three-state curve, as the intermediate was not well sampled under these conditions. However, the native baseline only begins to slope after ~ 0.5 M GdnHCl. This corresponds with the

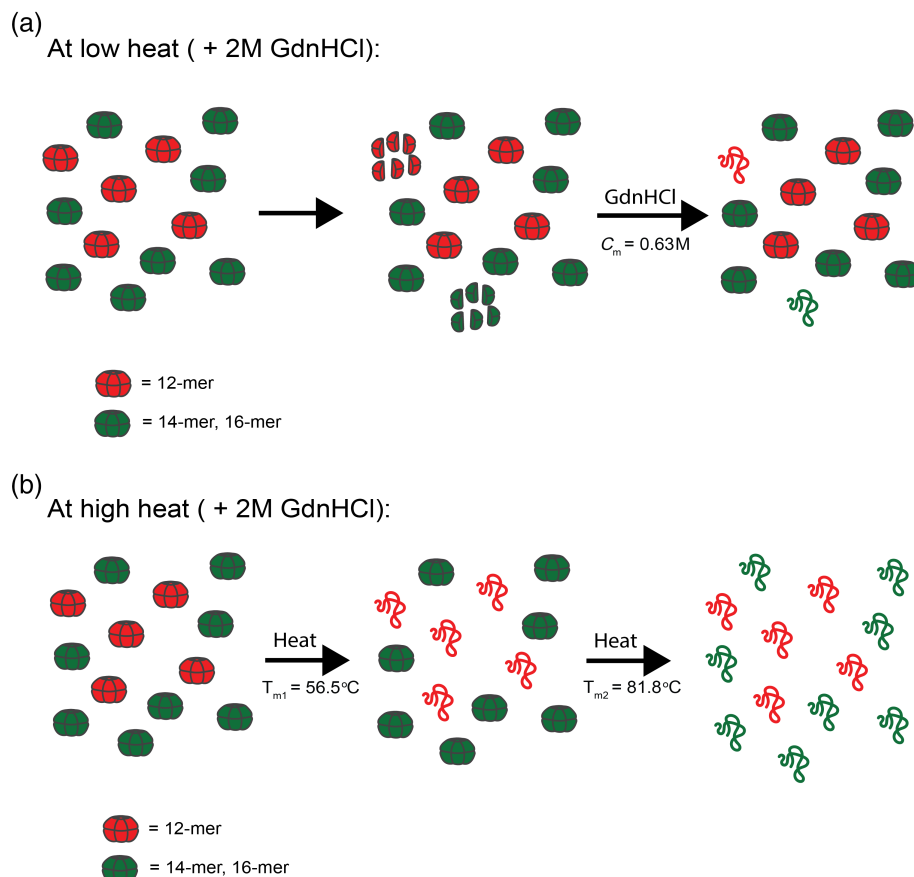


FIGURE 4 Schema of proposed mechanism of unfolding for CaMKII β hub oligomer during temperature melts in the presence of 2 M guanidine hydrochloride (GdnHCl). (a) At low heat, some oligomers disassemble into dimers regardless of stoichiometry. The dimers immediately unfold. (b) At high heat, 12-mers first disassemble and unfold in a cooperative transition. The 14- and 16-mers disassemble and unfold in a second cooperative transition. CAMKII, Ca²⁺/calmodulin-dependent protein kinase II.

C_m of the CaMKII β hub dimer (~ 0.6 M), indicating that dimers are unfolding at this point, likely because of oligomer dissociation. There are two visible transitions, one around 3 M GdnHCl and a second around 4.5 M GdnHCl. These transitions likely represent the same processes we visualized in the temperature + GdnHCl denaturation melts.

It is clear from both crystallography and EM studies that CaMKII holoenzymes and hub domains can adopt different stoichiometries. This adds to the complexity of this enzyme, which can form heterooligomeric complexes, and also adopt mixed oligomeric states of heterooligomers. The physiological relevance of these differences remains unclear, but will be important to interrogate moving forward. It is possible that the allowance of multiple stoichiometries facilitates subunit exchange between CaMKII holoenzymes (Bhattacharyya et al., 2016; Stratton et al., 2014). Our study has provided clear evidence that, despite nearly identical sequences, CaMKII α and β hub domains adopt different stoichiometries in solution and have distinct stabilities (Figure S8). This provides a framework for assessing the differences observed in activation and regulation between CaMKII α and β holoenzymes and how they may be related to dynamics and stability. Before addressing such questions, it would be necessary to determine whether full-length

CaMKII holoenzymes exhibit the same stoichiometries and disassembly properties as those observed here in hub domain holoenzymes.

4 | MATERIALS AND METHODS

4.1 | Protein purification

The CaMKII β full-length hub domain (residues 534–666) was expressed in Protein deficient B strain (BL21 DE3) cells with a N-terminal hexahistidine tag. The cells were induced at 18°C by adding 1 mM Isopropyl β -D-1-thiogalactopyranoside (IPTG) and grown overnight. The cells were resuspended in Buffer A (25 mM Tris-HCl pH 8.5, 150 mM KCl, 40 mM imidazole, and 10% glycerol), supplemented with commercially available protease inhibitors (0.5 mM benzamidine, 0.2 mM 4-(2-aminoethyl)benzenesulfonyl fluoride hydrochloride, 0.1 mg/mL trypsin inhibitor, 0.005 mM leupeptin, 1 μ g/mL pepstatin), 1 μ g/mL DNase/50 mM MgCl₂ were added, and the cells were then lysed. All subsequent steps were performed at 4°C using an ÄKTA pure chromatography system (GE). Cell lysate was loaded onto 5 mL His Trap FF Ni Sepharose column (GE) and eluted with 50% Buffer B (25 mM Tris-HCl pH 8.5, 150 mM KCl, 1 M

imidazole, 10% glycerol). The protein was desalted from excess imidazole using a HiPrep 26/10 Desalting column using Buffer C (25 mM Tris-HCl pH 8.8, 150 mM KCl, 1 mM EDTA, 2 mM DTT, and 10% glycerol). The hexahistidine tag was cleaved with PreScission protease overnight at 4°C. Proteins were eluted from HiTrap Q-FF with a step-gradient from 0% to 17% using Buffer BQ (25 mM Tris-HCl pH 8.5, 1 M KCl, 10% glycerol). Eluted proteins were concentrated and further purified using a Superose 6 size-exclusion column equilibrated with gel filtration buffer (25 mM Tris-HCl pH 8.0, 150 mM KCl, 1 mM Tris(2-carboxyethyl)phosphine (TCEP), 10% glycerol). Fractions (>95% purity) were pooled, concentrated, flash frozen in liquid nitrogen, and stored at -80°C until needed.

The CaMKIIβ hub dimer variant was designed by modifying the wild type CaMKIIβ hub domain via two mutations: F585A and L622M (residue numbering based on full-length, non-spliced CaMKIIβ). The variant was expressed in BL21 DE3 cells with an N-terminal hexahistidine tag and purified using the same process as the wild type CaMKIIβ hub. During the size-exclusion step, a Superdex 75 size exclusion column was used.

4.2 | Crystallization, data collection, and structure determination

Protein crystals of 14- and 16-mer CaMKIIβ hub domain were grown in the same drop using hanging drop vapor diffusion at 20°C. The drops contained 1 μL of the well solution and 1 μL of 1.9 mM hub domain. The well solution was 0.1 M imidazole pH 7, 0.15 DL-Malic acid pH 7 and 22% Polyethylene glycol (PEG) methyl ether 550. Crystals were frozen directly from the well solution. Diffraction data were collected at a wavelength of 1.5418 Å using a Rigaku MicroMax-007 HF X-ray source, which was coupled to a Rigaku VariMax HF optic system (UMass Amherst). The X-ray data were collected at 100 K. The datasets were integrated, merged scaled using HKL-2000. The structure was solved by molecular

replacement with Phaser (McCoy et al., 2007) using single CaMKIIγ hub domain (PDB: 2UX0) (Rellos et al., 2010) as the search model. Model building was performed using Coot and the refinement was carried out with Refmac5 (Murshudov et al., 2011).

4.3 | Guanidine melts

Two solutions of 10 μM CaMKIIβ hub were prepared, containing either 0 M GdnHCl or 6 M GdnHCl. All protein dilutions were performed using a modified gel filtration buffer suitable for CD (5 mM Tris-HCl pH 8.0, 150 mM KCl, 1 mM TCEP). A stock 6.5 M GdnHCl solution was used (6.5 M GdnHCl, 5 mM Tris-HCl pH 8.0, 150 mM KCl, 1 mM TCEP) to prepare GdnHCl solutions. The two solutions were titrated together to give an array of 10 μM CaMKIIβ hub solutions with a range of GdnHCl concentration. For the CaMKIIβ hub oligomer, these solutions ranged from 0 M to 6 M GdnHCl at steps of 0.33 M. For the CaMKIIβ hub dimer, these solutions range from 0 M to 1.15 M in 0.05 M steps.

Following the titration, protein samples were incubated for 20 min (CaMKIIβ hub oligomer) or 50 min (CaMKIIβ hub dimer). After equilibration, the extent of unfolding in each solution was measured on a Jasco J1500 CD spectrophotometer using 1 mm cuvettes. This was measured using CD signal. For each sample, the average CD at 218 nm was recorded over 30 s at 25°C. Additionally, full spectrum scans (195–260 nm) were recorded for CaMKIIβ hub oligomer and dimer samples in 0 M GdnHCl. The raw CD signal (mdegs) was converted to molar ellipticity (θ) for the full spectrum scans via the following conversion: $\theta = \text{mdegs} \times M / (10 \times L \times C)$, where M is average molecular weight in g/mol, L is path length of the cell, and C is concentration in grams per liter.

Using a non-linear regression, data were fitted to a two-state curve (Equation (1)) in Graph Pad Prism. The parameter values were used to calculate C_m values ($C_m = m4/m5$).

$$\theta = \frac{\theta_N + \theta_I \times e^{-\frac{(\Delta G_{\text{H}_2\text{O,NI}}^0 - m_{\text{NI}} \times [\text{GdnHCl}])}{RT}} + \theta_U \times e^{-\frac{(\Delta G_{\text{H}_2\text{O,NI}}^0 - m_{\text{NI}} \times [\text{GdnHCl}])}{RT}} \times e^{-\frac{(\Delta G_{\text{H}_2\text{O,IU}}^0 - m_{\text{IU}} \times [\text{GdnHCl}])}{RT}}}{1 + e^{-\frac{(\Delta G_{\text{H}_2\text{O,NI}}^0 - m_{\text{NI}} \times [\text{GdnHCl}])}{RT}} + e^{-\frac{(\Delta G_{\text{H}_2\text{O,NI}}^0 - m_{\text{NI}} \times [\text{GdnHCl}])}{RT}} \times e^{-\frac{(\Delta G_{\text{H}_2\text{O,IU}}^0 - m_{\text{IU}} \times [\text{GdnHCl}])}{RT}}}. \quad (1)$$

4.4 | Temperature melts

Protein samples of 60 μM CaMKII β hub and 2 M GdnHCl were prepared at a final volume of 215 μL . CD measurements were performed using a Jasco J1500 CD spectrophotometer. Protein samples in a 1 mm cuvette were heated from 20°C to 100°C at a rate of 0.67°C per minute. Every 1°C, the CD signal at 218 nm was recorded over 30 s. Full spectrum CD scans (205 to 260 nm) were taken every 10°C. Eight temperature melt replicates were performed. Using a nonlinear regression, data were fitted using Equation (2) in GraphPad Prism, where N is the native protein, I is the intermediate, U is the unfolded protein, NI is the first transition, and IU is the second transition. The average m_4 , m_5 , m_6 , and m_7 values were calculated over all replicates. These values were used to calculate the melting temperature for each transition ($T_{m,1} = m_4/m_5$ and $T_{m,2} = m_6/m_7$) and unfolding energies ($m_4 \times RT$ and $m_6 \times RT$, respectively) ($T = 297$ K).

$$\theta = \frac{\theta_N + \theta_I \times e^{\frac{-(\Delta G_{app,NI} - slope_{NI} \times T)}{RT}} + \theta_U \times e^{\frac{-(\Delta G_{app,NI} - slope_{NI} \times T)}{RT}} \times e^{\frac{-(\Delta G_{app,IU} - slope_{IU} \times T)}{RT}}}{1 + e^{\frac{-(\Delta G_{app,NI} - slope_{NI} \times T)}{RT}} + e^{\frac{-(\Delta G_{app,NI} - slope_{NI} \times T)}{RT}} \times e^{\frac{-(\Delta G_{app,IU} - slope_{IU} \times T)}{RT}}}. \quad (2)$$

4.5 | Mass photometry

All mass photometry measurements were performed on a Refeyn One MP mass photometer. All protein solutions were prepared in a filtered buffer (25 mM Tris-HCl pH 8.0, 150 mM KCl). Before each experiment, the buffer alone was measured as a control. The buffer was considered clean if the hit count was below 75. For each experiment, a standard mass calibration curve was calculated using Thyroglobulin (Tg) at 25 nM (final concentration on the coverslip), apoferritin (440 kDa) at 3.75 nM, and Bovine serum albumin (BSA) (66.5 kDa) at 15 nM; 5 μL of standard protein was added to 15 μL of MP buffer on a coverslip, and the MP was measured for 60 s.

For each run, a 200 μL solution of 2 μM protein and 2 M GdnHCl was prepared. The GdnHCl solution was filtered using a 0.22 μm filter before use. The sample was heated to the chosen temperatures using a thermocycler. The sample was held at each temperature for 90 s, at the end of which 6 μL were taken and immediately diluted onto the coverslip with 14 μL of MP buffer to perform an MP measurement over 60 s. Mass histograms of each run

were generated using Refeyn's DiscoverMP software ($n = 6$ for CaMKII α hub, $n = 8$ for CaMKII β hub).

4.6 | Size-exclusion chromatography multiangle light scattering

Size-exclusion chromatography (SEC) coupled with multiangle light scattering (MALS) was performed using an Agilent 1260 HPLC system, a DAWN HELEOS II MALS detector, and an Optilab-T-REX refractive index detector. The SEC column used was a Tosoh TSKGel G3000 SWxl (particle size 5 μm , 30 cm length, calibration range 10–500 kDa) and was equilibrated with ethanol, distilled water, and finally gel filtration buffer (25 mM Tris-HCl pH 8.0, 150 mM KCl, 1 mM TCEP, 10% glycerol). The SEC-MALS was conducted at a constant flow rate of 0.9 $\mu\text{L}/\text{min}$ with an injection volume of 50 μL to ensure accurate separation. Protein samples of CaMKII β hub oligomer and dimer were injected at a concentration of

262 mg/mL. The column temperature was maintained at 25°C throughout the analysis to prevent temperature-induced variations. Data were acquired and processed using ASTRA. The scattering data were analyzed based on the Zimm plot method to determine the molecular weight of the samples. The SEC-MALS system was calibrated using BSA (2 mg/mL) to ensure accurate determination of molecular weights.

AUTHOR CONTRIBUTIONS

Margaret M. Stratton: Conceptualization; investigation; funding acquisition; writing – original draft; methodology; writing – review and editing; formal analysis; project administration; supervision; visualization. **Can Özden:** Conceptualization; investigation; writing – original draft; methodology; validation; visualization; writing – review and editing; formal analysis; data curation. **Sara MacManus:** Conceptualization; investigation; writing – original draft; methodology; validation; visualization; writing – review and editing; formal analysis; data curation. **Ruth Adafia:** Investigation; methodology; validation; visualization; data curation. **Alfred**

Samkutty: Visualization; data curation. **Ana Torres Ocampo:** Visualization; data curation. **Scott C. Garman:** Formal analysis; visualization; supervision; methodology.



ACKNOWLEDGMENTS

We thank Stewart Loh and Alejandro Heuck for thoughtful comments on the project. We thank Eddie Esposito for help with DSC experiments. CD and SEC-MALS data were collected at the UMass Amherst Mass Biophysical Characterization Core Facility, RRID:SCR_022357.

CONFLICT OF INTEREST STATEMENT

The authors declare no conflicts of interest.

ORCID

Can Özden  <https://orcid.org/0000-0002-5673-878X>
Margaret M. Stratton  <https://orcid.org/0000-0003-2686-9022>

REFERENCES

- Bhattacharyya M, Karandur D, Kuriyan J. Structural insights into the regulation of Ca(2+)/Calmodulin-dependent protein kinase II (CaMKII). *Cold Spring Harb Perspect Biol.* 2019;12:a035147. <https://doi.org/10.1101/cshperspect.a035147>
- Bhattacharyya M, Stratton MM, Going CC, McSpadden ED, Huang Y, Susa AC, et al. Molecular mechanism of activation-triggered subunit exchange in Ca2+/ calmodulin-dependent protein kinase II. *Elife.* 2016;5:e13405. <https://doi.org/10.7554/eLife.13045>
- Buonarati OR, Miller AP, Coultrap SJ, Bayer KU, Reichow SL. Conserved and divergent features of neuronal CaMKII holoenzyme structure, function, and high-order assembly. *Cell Rep.* 2021;37:110168. <https://doi.org/10.1016/j.celrep.2021.110168>
- Chao LH, Stratton MM, Lee IH, Rosenberg OS, Levitz J, Mandell DJ, et al. A mechanism for tunable autoinhibition in the structure of a human Ca2+/calmodulin-dependent kinase II holoenzyme. *Cell.* 2011;146:732–45. <https://doi.org/10.1016/j.cell.2011.07.038>
- Hoelz A, Nairn AC, Kuriyan J. Crystal structure of a tetradecameric assembly of the association domain of Ca2+/calmodulin-dependent kinase II. *Mol Cell.* 2003;11:1241–51.
- Hoffman L, Stein RA, Colbran RJ, McHaourab HS. Conformational changes underlying calcium/calmodulin-dependent protein kinase II activation. *EMBO J.* 2011;30:1251–62. <https://doi.org/10.1038/emboj.2011.40>
- Kolodziej SJ, Hudmon A, Waxham MN, Stoops JK. Three-dimensional reconstructions of calcium/calmodulin-dependent (CaM) kinase IIalpha and truncated CaM kinase IIalpha reveal a unique organization for its structural core and functional domains. *J Biol Chem.* 2000;275:14354–9. <https://doi.org/10.1074/jbc.275.19.14354>
- Leurs U, Klein AB, McSpadden ED, Griem-Krey N, Solbak SMO, Houlton J, et al. GHB analogs confer neuroprotection through specific interaction with the CaMKIIalpha hub domain. *Proc Natl Acad Sci U S A.* 2021;118:e2108079118. <https://doi.org/10.1073/pnas.2108079118>
- Lucic I, Heluin L, Jiang PL, Castro Scalise AG, Wang C, Franz A, et al. CaMKII autophosphorylation can occur between holoenzymes without subunit exchange. *Elife.* 2023;12:e86090. <https://doi.org/10.7554/eLife.86090>
- McCoy AJ, Grosse-Kunstleve RW, Adams PD, Winn MD, Storoni LC, Read RJ. Phaser crystallographic software. *J Appl Cryst.* 2007;40:658–74. <https://doi.org/10.1107/S0021889807021206>
- McSpadden ED, Xia Z, Chi CC, Susa AC, Shah NH, Gee CL, et al. Variation in assembly stoichiometry in non-metazoan homologs of the hub domain of Ca(2+)/calmodulin-dependent protein kinase II. *Protein Sci.* 2019;28:1071–82. <https://doi.org/10.1002/pro.3614>
- Morris EP, Torok K. Oligomeric structure of alpha-calmodulin-dependent protein kinase II. *J Mol Biol.* 2001;308:1–8. <https://doi.org/10.1006/jmbi.2001.4584>
- Murshudov GN, Skubak P, Lebedev AA, Pannu NS, Steiner RA, Nicholls RA, et al. REFMAC5 for the refinement of macromolecular crystal structures. *Acta Crystallogr D Biol Crystallogr.* 2011;67:355–67. <https://doi.org/10.1107/S0907444911001314>
- Rellos P, Pike AC, Niesen FH, Salah E, Lee WH, von Delft F, et al. Structure of the CaMKIIdelta/calmodulin complex reveals the molecular mechanism of CaMKII kinase activation. *PLoS Biol.* 2010;8:e1000426. <https://doi.org/10.1371/journal.pbio.1000426>
- Roman Sloutsky ND, Dunn MJ, Bates RM, Torres-Ocampo AP, Boopathy S, Page B, et al. Heterogeneity in human hippocampal CaMKII transcripts reveals allosteric hub-dependent regulation. *Sci Signal.* 2020;13:eaaz0240.
- Rosenberg OS, Deindl S, Comolli LR, Hoelz A, Downing KH, Nairn AC, et al. Oligomerization states of the association domain and the holoenzyme of Ca2+/CaM kinase II. *FEBS J.* 2006;273:682–94.
- Saha S, Ozden C, Samkutty A, Russi S, Cohen A, Stratton MM, et al. Polymer-based microfluidic device for on-chip counter-diffusive crystallization and in situ X-ray crystallography at room temperature. *Lab Chip.* 2023;23:2075–90. <https://doi.org/10.1039/d2lc01194h>
- Sarkar P, Davis KA, Puhl HL, Veetil JV, Nguyen TA, Vogel SS. Deciphering CaMKII Multimerization using fluorescence correlation spectroscopy and homo-FRET analysis. *Biophys J.* 2017;112:1270–81. <https://doi.org/10.1016/j.bpj.2017.02.005>
- Sloutsky R, Stratton MM. Functional implications of CaMKII alternative splicing. *Eur J Neurosci.* 2020;54:6780–94.
- Sonn-Segev A, Belacic K, Bodrug T, Young G, VanderLinden RT, Schulman BA, et al. Quantifying the heterogeneity of macromolecular machines by mass photometry. *Nat Commun.* 2020;11:1772. <https://doi.org/10.1038/s41467-020-15642-w>
- Stratton M, Lee IH, Bhattacharyya M, Christensen SM, Chao LH, Schulman H, et al. Activation-triggered subunit exchange between CaMKII holoenzymes facilitates the spread of kinase activity. *Elife.* 2014;3:e01610. <https://doi.org/10.7554/eLife.01610>
- Tombes RM, Faison MO, Turbeville JM. Organization and evolution of multifunctional Ca(2+)/CaM-dependent protein kinase genes. *Gene.* 2003;322:17–31.
- Torres-Ocampo AP, Ozden C, Hommer A, Gardella A, Lapinskas E, Samkutty A, et al. Characterization of CaMKII alpha

holoenzyme stability. *Protein Sci.* 2020;29:1524–34. <https://doi.org/10.1002/pro.3869>

Young G, Hundt N, Cole D, Fineberg A, Andrecka J, Tyler A, et al. Quantitative mass imaging of single biological macromolecules. *Science.* 2018;360:423–7.

SUPPORTING INFORMATION

Additional supporting information can be found online in the Supporting Information section at the end of this article.

How to cite this article: Özden C, MacManus S, Adafia R, Samkutty A, Torres-Ocampo AP, Garman SC, et al. Ca²⁺/CaM dependent protein kinase II (CaMKII) α and CaMKII β hub domains adopt distinct oligomeric states and stabilities. *Protein Science.* 2024;33(4):e4960. <https://doi.org/10.1002/pro.4960>